Research Square

Preprints are preliminary reports that have not undergone peer review.
They should not be considered conclusive, used to inform clinical practice,
or referenced by the media as validated information.

Preoperative Aerobic Exercise Training Protects Against Hepatic Ischemia–Reperfusion Injury Through the MG53–CAV-1 Axis

Xue Xiao
Third Affiliated Hospital of Sun Yat-sen University
Xinmin Zhang
First Hospital of Jilin University
Kexin Hu
Third Affiliated Hospital of Sun Yat-sen University
Jinyan Guo
Third Affiliated Hospital of Sun Yat-sen University
Xiaotong Li
Third Affiliated Hospital of Sun Yat-sen University
Xueyou Jiang
Third Affiliated Hospital of Sun Yat-sen University
Jun Liu
Third Affiliated Hospital of Sun Yat-sen University
Ziqing Hei
Third Affiliated Hospital of Sun Yat-sen University
Zhongqi Liu
Sun Yat-sen Memorial Hospital
Xue Han
hanx39@mail.sysu.edu.cn

Sun Yat-sen Memorial Hospital

Research Article

Keywords: hepatic ischemia–reperfusion injury, aerobic exercise training, MG53, Caveolin-1, ferroptosis

Posted Date: November 5th, 2026

DOI: https://doi.org/10.21203/rs.3.rs-11372556/v1

License: This work is licensed under a Creative Commons Attribution 4.0 International License.
Read Full License

Additional Declarations: No competing interests reported.

Preoperative Aerobic Exercise Training Protects Against Hepatic Ischemia–Reperfusion Injury Through the MG53–CAV-1 Axis

Abstract

Background: Hepatic ischemia–reperfusion injury (HIRI) remains a significant clinical challenge in liver surgery and transplantation. Although aerobic exercise training (AET) confers systemic benefits, the mechanisms by which it mitigates HIRI remain poorly defined.

Methods: Male C57BL/6 mice underwent sedentary housing or 5 weeks of moderate-intensity swimming training before partial hepatic I/R. Liver injury, oxidative stress, apoptosis, iron homeostasis, ferroptosis-associated markers, and hepatic MG53–Caveolin-1 (CAV-1) signaling were evaluated. Hepatic MG53 was silenced using hydrodynamically delivered Ad-shMG53, and TAT–MG53 was administered via the portal vein at the onset of reperfusion. CAV-1-dependent signaling was pharmacologically disrupted with Daidzein.

Results: Preoperative AET significantly reduced serum ALT and AST, alleviated oxidative stress, and suppressed ferroptotic markers following HIRI. AET increased hepatic MG53 expression, enhanced MG53–Caveolin-1 interaction, and preserved cellular redox homeostasis. MG53 knockdown abolished AET–associated hepatoprotection, whereas TAT–MG53 supplementation restored protective phenotypes. Disruption of Caveolin-1 abrogated the benefits of AET and TAT–MG53 following HIRI.

Conclusions: Preoperative AET protects against HIRI through an MG53–CAV-1-dependent mechanism that preserves hepatic iron and redox homeostasis and limits oxidative and ferroptosis-associated injury. The MG53–CAV-1 axis may represent a potential perioperative therapeutic target for reducing liver I/R injury.

Keywords: hepatic ischemia–reperfusion injury; aerobic exercise training; MG53; Caveolin-1; ferroptosis

1. Introduction

Hepatic ischemia–reperfusion injury (HIRI) is a major cause of liver dysfunction after liver resection and transplantation [1]. Although restoration of blood flow is essential for tissue survival, reperfusion can amplify ischemic damage by triggering oxidative stress, inflammatory signaling, and regulated cell death [2, 3]. Ferroptosis, an iron-dependent form of cell death driven by lipid peroxidation, has emerged as an important contributor to HIRI. Experimental inhibition of ferroptosis or its upstream regulators attenuates hepatic injury in models of warm I/R and fatty-liver I/R, supporting a functional link between iron dysregulation, lipid peroxidation, and reperfusion injury [5-7]. However, effective strategies that enhance intrinsic hepatic resistance to I/R remain limited.

Preoperative exercise training is a potentially feasible, nonpharmacological strategy for improving resistance to surgical stress [8, 9]. In mice, preoperative exercise training reduced hepatic I/R injury, tissue necrosis, neutrophil infiltration, and neutrophil extracellular trap formation, indicating coordinated effects on both tissue resilience and inflammatory responses [10]. More recently, exercise preconditioning of donor mice was shown to reduce cold I/R injury following liver transplantation or ex vivo reperfusion, extending the protective effect of exercise to a clinically relevant transplantation setting [11]. Nevertheless, the molecular mechanisms through which preoperative exercise enhances hepatic stress tolerance remain poorly understood.

MG53, also known as TRIM72, is a membrane-repair protein enriched in striated muscle that regulates vesicle trafficking and the recruitment of repair machinery to sites of membrane damage [12, 13]. Following membrane injury, MG53 rapidly accumulates at damaged sites and facilitates membrane resealing, thereby limiting cellular damage [12,14]. Recombinant MG53 has been shown to reduce hepatocellular membrane injury, oxidative stress, and apoptosis in experimental hepatic I/R, supporting a protective role for MG53 beyond skeletal and cardiac muscle [15]. Caveolin-1 (CAV-1), the principal scaffolding protein of caveolae, regulates membrane organization and cellular stress responses. Genetic loss of CAV-1 aggravates hepatic I/R injury, whereas hepatocyte CAV-1 contributes to ferritin-dependent iron storage and protection against iron-mediated oxidative stress [16, 17]. Importantly, MG53 has been shown to associate with CAV-1 and regulate caveolar endocytosis in lung epithelial cells, providing biological plausibility for functional cooperation between these membrane-repair proteins [18]. Whether this relationship operates in the liver and contributes to exercise-induced protection against HIRI has not been determined.

In the present study, we investigated whether MG53 is required for the hepatoprotective effects of preoperative aerobic exercise training and whether CAV-1 contributes to MG53-dependent protection. Using liver-directed MG53 knockdown, TAT–MG53 rescue, and pharmacological perturbation of CAV-1, we evaluated liver injury, oxidative stress, apoptosis, iron and redox homeostasis, and ferroptosis-associated molecular changes after hepatic I/R. We hypothesized that

preoperative exercise enhances hepatic resistance to I/R through a protective mechanism involving MG53 and CAV-1.

2. Materials & Methods

2.1. Animals

Male C57BL/6 mice (8–10 weeks old; 25.16 ± 1.72 g) were housed under specific pathogen-free conditions (24 ± 2 °C, 50% humidity, 12-h light/dark cycle) with free access to food and water and acclimatized for 1 week before experiments. All animal experiments were performed in accordance with the National Institutes of Health Guide for the Care and Use of Laboratory Animals and were approved by the Animal Ethics Committee.

2.2. Experimental Design

To evaluate the effects of preoperative aerobic exercise training (AET) on hepatic ischemia–reperfusion injury (HIRI), mice were randomly assigned to sedentary or AET groups (n = 14/group). After 5 weeks, each group was further divided into sham and HIRI subgroups (n = 7/group). Mice in the HIRI groups underwent partial hepatic ischemia–reperfusion surgery, whereas sham-operated mice underwent the same procedure without vascular occlusion.

To assess the role of MG53, mice were randomly assigned to Sedentary, AET, Ad-shNeg, Ad-shMG53, and Ad-shMG53+TAT-MG53 groups (n = 5–7/group).

Except for the sedentary group, mice underwent the 5-week swimming protocol. Fourteen days before surgery, Ad-shMG53 or control adenovirus was administered by hydrodynamic tail-vein injection. At reperfusion, mice in the Ad-shMG53+TAT-MG53 group received TAT-MG53 (6.0 mg/kg) via the portal vein.

To investigate the role of Caveolin-1 (CAV-1), mice were assigned to Sedentary, AET, TAT-MG53, AET+Daidzein, and TAT-MG53+Daidzein groups (n = 5–7/group). Daidzein (0.8 mg/kg/day, i.p.) was administered for 7 consecutive days before surgery in the indicated groups. TAT-MG53 (6.0 mg/kg) was injected via the portal vein at reperfusion.

2.3. AET Protocol

Swimming was used as the preoperative AET model [19]. Mice were trained in a Plexiglas tank filled with water (30 ± 2 °C) for 5 weeks. During the first week, swimming duration was gradually increased from 10 to 50 min/day for adaptation. From week 2 onward, mice underwent formal training for 50 min/day, 6 days/week. Sedentary mice were housed under the same conditions without exercise.

2.4. HIRI Model

A 70% partial hepatic ischemia model was established. After 12 h of fasting, mice underwent midline laparotomy under anesthesia. The portal vein and hepatic artery supplying the left lateral and median lobes were occluded with atraumatic clips for 60 min, followed by clip removal to initiate reperfusion. Sham-operated mice underwent

the same surgical exposure without vascular clamping. After 6 h of reperfusion, blood and liver tissues were collected for biochemical, histological, and molecular analyses.

2.5. Assessment of oxidative stress and ferroptosis-related parameters

Hepatic oxidative stress was evaluated by measuring malondialdehyde (MDA), 15-F_{2t}-isoprostane, and superoxide dismutase (SOD) activity. Hepatic iron overload was assessed by quantifying Fe^{2+} and Fe^{3+} levels in liver homogenates and by Prussian blue staining. Redox homeostasis was further assessed by determining hepatic GSH/GSSG and NADPH/$NADP^+$ ratios. Hepatic GPX4 and serum MG53 levels were quantified by ELISA [20].

2.6. MG53 knockdown and TAT-MG53 administration

Recombinant adenoviruses encoding MG53 shRNA (Ad-shMG53) or control shRNA (Ad-shNeg) were delivered by hydrodynamic tail-vein injection for hepatic gene silencing [21]. TAT-MG53 fusion protein was prepared as previously described and administered via portal-vein injection at reperfusion. Details of viral constructs, protein preparation, biodistribution, and biosafety evaluation are provided in the Supplementary Methods.

2.7. Serum biochemical analysis

Serum ALT and AST levels were quantified using a fully automated biochemistry analyzer in accordance with the manufacturer's instructions.

2.8. Histological and fluorescence staining

Liver injury was assessed by hematoxylin and eosin (H&E) staining and scored using Suzuki's criteria. Reactive oxygen species (ROS) generation was evaluated by dihydroethidium (DHE) staining. Apoptosis was assessed by TUNEL staining. Iron deposition was visualized by Prussian blue staining. Fluorescence and histological images were acquired under identical settings and quantified using ImageJ or Image-Pro Plus software.

2.9. Western Blotting

Liver tissues were lysed in RIPA buffer containing protease inhibitors. Equal amounts of protein were separated by SDS–PAGE and transferred to PVDF membranes. After blocking, membranes were incubated with primary antibodies overnight at 4 °C, followed by HRP-conjugated secondary antibodies. Protein bands were visualized by enhanced chemiluminescence and quantified using ImageJ. Relative protein expression was normalized to GAPDH. Detailed antibody information is listed in **Supplementary Table S1**.

2.10. RT-qPCR

Total RNA was extracted from liver tissue using TRIzol reagent and reverse-transcribed into cDNA. Quantitative PCR was performed using gene-specific primers on a LightCycler 480 system. Relative mRNA expression was calculated using the $2^{\wedge-\Delta\Delta Ct}$ method with Gapdh as the internal control. Primer sequences are provided in the Supplementary Methods.

2.11. Co-immunoprecipitation

Co-immunoprecipitation was performed using liver lysates according to the manufacturer's instructions. Briefly, clarified lysates were incubated with anti-MG53 or anti-CAV-1 antibodies overnight at 4 °C, followed by capture with protein A/G beads. Immunoprecipitated proteins were analyzed by Western blotting.

2.12. Statistical Analysis

Data are presented as mean ± SD. Statistical analyses were performed using GraphPad Prism 9.0. Comparisons in Experiment 1 were analyzed by two-way ANOVA followed by Šídák's multiple comparisons test [22]. Comparisons among multiple groups in Experiments 2 and 3 were analyzed by one-way ANOVA followed by Holm–Šídák multiple comparisons test. Non-normally distributed data were analyzed using the Kruskal–Wallis test. A two-sided $P < 0.05$ was considered statistically significant.

3. Result

3.1 Preoperative AET Protects Against HIRI by Attenuating Oxidative Stress and Apoptotic Cell Death

Mice underwent a 5-week swimming-based aerobic exercise training (AET) protocol before hepatic ischemia–reperfusion (I/R) surgery **(Fig. 1A)**. Food intake, rest–activity patterns, and body weight were comparable between sedentary and

AET-trained mice throughout the training period **(Fig. S1),** indicating that the protocol was well tolerated.

Hepatic I/R markedly increased serum AST and ALT levels and caused extensive histopathological injury, including sinusoidal congestion, inflammatory infiltration, hepatocellular necrosis, and cytoplasmic vacuolization **(Fig. 1B–1E)**. Preoperative AET significantly reduced serum transaminase levels, improved hepatic architecture, and decreased Suzuki injury scores **(Fig. 1B–1E)**.

AET also reduced oxidative stress and apoptotic cell death after hepatic I/R. DHE fluorescence and the number of TUNEL-positive hepatocytes were significantly decreased in AET-trained mice **(Fig. 1F–1 I)**. In addition, AET reduced hepatic 15-F_{2t}-isoprostane and MDA levels while preserving SOD activity **(Fig. 1J–1L)**. Collectively, these findings show that preoperative AET protects against acute HIRI by attenuating oxidative stress, lipid peroxidation, and hepatocyte apoptosis.

3.2 Preoperative AET Attenuates Ferroptosis-Associated Iron Accumulation and Redox Imbalance During HIRI

Because iron accumulation and lipid peroxidation are key features of ferroptosis, we next examined hepatic iron and redox status after I/R. Prussian blue staining showed minimal iron deposition in sham livers but marked accumulation in HIRI livers, which was significantly reduced by preoperative AET **(Fig. 2A)**. Consistently,

AET decreased both total hepatic iron and ferrous iron (Fe^{2+}) levels after HIRI **(Fig. 2B, 2C)**.

AET also improved hepatic redox homeostasis, as evidenced by increased GSH levels and higher GSH/GSSG and NADPH/$NADP^+$ ratios **(Fig. 2D–2F)**. At the molecular level, HIRI reduced GPX4 expression and increased the ferroptosis-associated proteins ALOX12 and ACSL4, while decreasing the iron-storage protein FTH1. These changes were partially reversed by AET **(Fig. 2G–2K)**. Collectively, these findings indicate that preoperative AET limits hepatic iron accumulation, preserves redox balance, and attenuates ferroptosis-associated molecular changes following HIRI.

3.3 MG53 Is Essential for AET-Mediated Hepatoprotection Against HIRI

To investigate whether MG53 contributes to the protective effects of preoperative AET, we first examined hepatic MG53 expression after HIRI. AET significantly increased hepatic MG53 protein levels in mice subjected to I/R, whereas no appreciable difference was observed between the sham groups **(Fig. 3A, 3B)**.

To assess the functional role of MG53, hepatic MG53 was silenced by hydrodynamic delivery of Ad-shMG53 14 days before I/R. In the rescue group, TAT–MG53 fusion protein was administered via the hepatic portal vein immediately after reperfusion, as illustrated in Fig. 3C. Ad-shMG53 efficiently reduced MG53 expression in the liver without affecting MG53 levels in skeletal muscle, myocardium,

lung, or kidney **(Fig. S2A–S2C)**. Circulating MG53 levels were also reduced, whereas neither Ad-shNeg nor Ad-shMG53 caused detectable baseline liver injury **(Fig. S2D–S2I)**. TAT–MG53 showed rapid hepatic uptake, reaching a peak at 6–8 h after administration **(Fig. S3A–S3B)**. Based on its favorable safety profile, 6.0 mg/kg was selected for subsequent rescue experiments **(Fig. S3C, S3G)**.

Functionally, MG53 knockdown markedly attenuated the protective effects of AET during HIRI, as evidenced by increased serum AST and ALT levels, aggravated histopathological injury, and higher Suzuki scores **(Fig. 3D–3G)**. MG53 depletion also reversed the AET-mediated reductions in hepatic DHE fluorescence, TUNEL-positive hepatocytes, 15-F_{2t}-isoprostane, and MDA levels, while reducing the preservation of SOD activity **(Fig. 3H–3N)**. Importantly, TAT–MG53 administration at the onset of reperfusion substantially reversed these effects in MG53-deficient mice **(Fig. 3H–3N)**. Collectively, these findings establish MG53 as an essential mediator of AET-induced hepatoprotection during acute HIRI.

3.4 MG53 Mediates the Protective Effects of AET on Hepatic Iron and Redox Homeostasis During HIRI

Having established that MG53 is essential for the overall hepatoprotective effects of AET, we next examined whether MG53 mediates the associated changes in hepatic iron and redox homeostasis. In AET-trained mice, hepatic MG53 knockdown abolished the AET-mediated reduction in iron accumulation, as demonstrated by increased Prussian blue–positive areas and elevated total hepatic iron and Fe^{2+} levels

after HIRI **(Fig. 4A–4C)**. These changes were substantially reversed by TAT–MG53 supplementation.

MG53 depletion also reversed the beneficial effects of AET on hepatic redox balance, leading to reduced GSH levels, lower GSH/GSSG and $NADPH/NADP^+$ ratios, and decreased GPX4 activity **(Fig. 4D–4G)**. In parallel, MG53 knockdown increased the ferroptosis-associated proteins ALOX12 and ACSL4 and decreased the iron-storage protein FTH1. TAT–MG53 largely restored this molecular profile **(Fig. 4H–4K)**. Collectively, these findings identify MG53 as a critical mediator of AET-induced maintenance of hepatic iron and redox homeostasis during HIRI and support its role in limiting ferroptosis-associated injury.

3.5 Preoperative AET Enhances the Hepatic MG53–CAV-1 Association During HIRI

Given the role of CAV-1 as a membrane-scaffolding protein involved in cellular stress adaptation, we investigated whether CAV-1 participates in MG53-mediated hepatoprotection during HIRI. Hepatic CAV-1 abundance was reduced after I/R in sedentary mice but was partially preserved by preoperative AET **(Fig. 5A, 5B)**.

Co-immunoprecipitation analysis demonstrated an association between MG53 and CAV-1 in liver tissue after HIRI. This association was enhanced by AET, weakened by hepatic MG53 knockdown, and restored by TAT–MG53

supplementation **(Fig. 5C, 5D)**, indicating that MG53 availability contributes to MG53–CAV-1 complex formation during I/R stress.

Both AET and TAT–MG53 increased hepatic MG53 and CAV-1 protein levels after HIRI. In contrast, pharmacological inhibition of CAV-1 with Daidzein reduced CAV-1 abundance but had little effect on MG53 expression **(Fig. 5E–5G)**. These findings suggest that CAV-1 availability may regulate MG53–CAV-1 complex formation without directly controlling MG53 expression, supporting a role for the MG53–CAV-1 axis in AET-mediated hepatoprotection.

3.6 Pharmacological Suppression of CAV-1 Abrogates AET- and MG53-Mediated Hepatoprotection Against HIRI

To determine whether CAV-1 is functionally required for AET- and MG53-mediated hepatoprotection, mice were pretreated with Daidzein for 7 consecutive days before HIRI, followed by portal-vein administration of TAT–MG53 at the onset of reperfusion **(Fig. 6A)**.

Preoperative AET and TAT–MG53 each markedly reduced serum AST and ALT levels, alleviated histopathological injury, and lowered Suzuki scores. These protective effects were largely lost following Daidzein pretreatment **(Fig. 6B–6E)**.

Consistent with these findings, Daidzein abolished the AET- and TAT–MG53-mediated reductions in hepatic DHE fluorescence, TUNEL-positive hepatocytes, 15-F_{2t}-isoprostane, and MDA levels, while reversing the preservation of

SOD activity **(Fig. 6F–6L)**. Collectively, these results suggest that intact CAV-1–dependent signaling is required for both exercise- and MG53-mediated protection against acute HIRI.

3.7 CAV-1 Suppression Reverses AET- and MG53-Mediated Improvements in Hepatic Iron and Redox Homeostasis During HIRI

Because CAV-1 was required for the overall hepatoprotective effects of AET and TAT–MG53, we next examined whether this dependency extended to ferroptosis-associated iron and redox alterations. Both AET and TAT–MG53 reduced hepatic iron deposition, total iron, and Fe^{2+} levels after HIRI. These effects were largely lost following Daidzein pretreatment **(Fig. 7A–7C**).

Similarly, AET and TAT–MG53 preserved hepatic redox homeostasis, as reflected by increased NADPH/$NADP^+$ and GSH/GSSG ratios, higher GSH levels, and preserved GPX4 activity. Daidzein pretreatment markedly attenuated these protective effects **(Fig. 7D–7G)**. At the molecular level, AET and TAT–MG53 decreased ALOX12 and ACSL4 expression while increasing FTH1 expression; these changes were largely reversed by Daidzein **(Fig. 7H–7K)**.

Collectively, these findings suggest that CAV-1–dependent signaling is required for the AET- and MG53-mediated preservation of hepatic iron and redox homeostasis and the attenuation of ferroptosis-associated injury during HIRI.

4. Discussion

This study demonstrates that preoperative aerobic exercise training (AET) attenuates acute hepatic ischemia–reperfusion injury (HIRI) through an MG53-dependent protective mechanism involving CAV-1. Previous studies showed that exercise preconditioning reduces hepatic necrosis, inflammation, and neutrophil extracellular trap formation after warm I/R and improves donor-liver tolerance to cold I/R [10,11]. Our findings extend these observations by linking exercise-induced hepatic protection to MG53–CAV-1-associated membrane and redox regulation.

MG53 is a stress-responsive membrane-repair protein that coordinates vesicle recruitment and membrane resealing following cellular injury [12,13,23,32]. Recombinant MG53 has previously been shown to reduce oxidative stress and hepatocyte apoptosis during hepatic I/R [15,33]. Here, hepatic MG53 knockdown markedly attenuated AET-induced protection, whereas TAT–MG53 administration at reperfusion restored the protective phenotype, supporting MG53 as a functional mediator of exercise-induced hepatoprotection. However, whether the increased hepatic MG53 reflects local production, enhanced uptake of circulating MG53, or altered protein stability remains unresolved [24,25,37].

CAV-1 organizes caveolar membrane domains and protects against oxidative, nitrative, and apoptotic injury during hepatic I/R [16,31]. AET preserved hepatic CAV-1 abundance and enhanced MG53–CAV-1 association, whereas MG53 knockdown weakened this association and TAT–MG53 restored it. Moreover, pharmacological

reduction of CAV-1 attenuated the protective effects of both AET and TAT–MG53 without substantially altering MG53 abundance, suggesting that CAV-1 provides a permissive membrane environment for MG53 function. Nevertheless, co-immunoprecipitation demonstrates protein association rather than direct binding, which requires further localization and interaction-domain studies [18].

The MG53–CAV-1 pathway was also associated with preserved hepatic iron and redox homeostasis. Iron overload and impaired GSH–GPX4 defense promote lipid peroxidation and increase susceptibility to hepatic I/R, whereas iron chelation or ferroptosis inhibition reduces liver injury [4–6,20,26,34–36]. The coordinated effects of AET, MG53 knockdown, TAT–MG53 rescue, and CAV-1 perturbation on iron accumulation, GPX4 activity, ACSL4, ALOX12, and FTH1 suggest that ferroptosis-associated injury is an important downstream component of this protective response [2,17,27]. However, because ferroptosis was not directly manipulated, these findings should be interpreted as attenuation of ferroptosis-associated changes rather than definitive inhibition of ferroptotic cell death.

These findings support exercise preconditioning as a potential strategy for enhancing hepatic resistance before elective surgery and TAT–MG53 as a possible intervention at reperfusion [10,11,15,33]. Several limitations should be considered, including the use of only male mice, assessment of a single acute reperfusion time point, and the absence of direct membrane-repair and ferroptosis-rescue experiments [28,29]. In addition, daidzein is not a highly selective CAV-1 inhibitor and may exert

CAV-1-independent effects, highlighting the need for hepatocyte-specific CAV-1 knockout and rescue studies [30].

In conclusion, preoperative AET protects against HIRI through an MG53-dependent pathway involving CAV-1, accompanied by improved iron and redox homeostasis and reduced ferroptosis-associated injury. These findings identify MG53–CAV-1 signaling as a potential mechanistic link between exercise adaptation and hepatic resistance to reperfusion stress.

5. Conclusion

In conclusion, our study identifies an AET–MG53–CAV-1 protective pathway in hepatic ischemia–reperfusion injury. Preoperative AET increased hepatic MG53 availability, enhanced its association with CAV-1, preserved iron and redox homeostasis, and attenuated oxidative, apoptotic, and ferroptosis-associated injury during reperfusion. Hepatic MG53 knockdown abolished these benefits, whereas TAT–MG53 administration at reperfusion restored them. Pharmacological disruption of CAV-1 weakened MG53–CAV-1 association and attenuated the protective effects of both AET and TAT–MG53, supporting an essential role for CAV-1-associated membrane organization in MG53-mediated hepatoprotection. These findings provide a mechanistic basis for exercise-induced hepatic protection and support AET and MG53-based therapy as potential perioperative strategies for reducing HIRI.

Abbreviations

HIRI	Hepatic ischemia–reperfusion injury
AET	aerobic exercise training
CAV-1	Caveolin-1
Ad-shMG53	adenoviral shRNA construct
MDA	malondialdehyde
SOD	superoxide dismutase
H&E	hematoxylin and eosin
DHE	dihydroethidium

Clinical trial number: not applicable.

[References]

[1] Hirao H, Nakamura K, Kupiec-Weglinski JW. Liver ischaemia-reperfusion injury: a new understanding of the role of innate immunity. Nat Rev Gastroenterol Hepatol. 2022, 19(4): 239-256.

[2] Zhang XJ, Cheng X, Yan ZZ, et al. An ALOX12-12-HETE-GPR31 signaling axis is a key mediator of hepatic ischemia-reperfusion injury. Nat Med. 2018;24(1):73-83.

[3] Marshall K, Jin J, Atkinson C, et al. Natural immunoglobulin M initiates an inflammatory response important for both hepatic ischemia reperfusion injury and regeneration in mice. Hepatology. 2018;67(2):721-735.

[4] Jia K, Zhang Y, Li F, et al. Acteoside ameliorates hepatocyte ferroptosis and hepatic ischemia-reperfusion injury via targeting PCBP2. Acta Pharm Sin B. 2025;15(4):2077-2094.

[5] Zhang Y, Wei H, Wang M, et al. Dexmedetomidine alleviates ferroptosis following hepatic ischemia-reperfusion injury by upregulating Nrf2/GPx4-dependent antioxidant responses. Biomed Pharmacother. 2023;169:115915.

[6] Rokop ZP, Zhang W, Ghosh N, et al. Exacerbated ischemia-reperfusion injury in fatty livers is mediated by lipid peroxidation stress and ferroptosis. Surgery. 2024;175(6):1539-1546.

[7] Liu J, Luo R, Zhang Y, et al. Current status and perspective on molecular targets and therapeutic intervention strategy in hepatic ischemia-reperfusion injury. Clin Mol Hepatol. 2024, 30(4):585-619.

[8] Wang Y, Luo D, Jiang H, et al. Effects of physical exercise on biomarkers of oxidative stress in healthy subjects: A meta-analysis of randomized controlled trials. Open Life Sci. 2023, 18(1):20220668.

[9] Xie Y, Gu Y, Li Z, et al. Effects of exercise on different antioxidant enzymes and related indicators: a systematic review and meta-analysis of randomized controlled trials. Sci Rep. 2025, 15(1):12518.

[10] Yazdani HO, Kaltenmeier C, Morder K, et al. Exercise Training Decreases Hepatic Injury and Metastases Through Changes in Immune Response to Liver Ischemia/Reperfusion in Mice. Hepatology. 2021;73(6):2494-2509.

[11] Yazdani HO, Yang R, Haykal T, et al. Exercise Preconditioning of the Donor Liver Decreases Cold Ischemia/Reperfusion Injury in a Mouse Model. Transplantation. 2025;109(1):161-173.

[12] Ma Y, Ding L, Li Z, et al. Structural basis for TRIM72 oligomerization during membrane damage repair. Nat Commun. 2023, 14(1):1555.

[13] Cai C, Masumiya H, Weisleder N, et al. MG53 regulates membrane budding and exocytosis in muscle cells. J Biol Chem. 2009;284(5):3314-3322.

[14] Gumpper-Fedus K, Park KH, Ma H, et al. MG53 preserves mitochondrial integrity of cardiomyocytes during ischemia reperfusion-induced oxidative stress. Redox Biol. 2022, 54:102357.

[15] Yao W, Li H, Han X, et al. MG53 anchored by dysferlin to cell membrane reduces hepatocyte apoptosis which induced by ischaemia/reperfusion injury in vivo and in vitro. J Cell Mol Med. 2017;21(10):2503-2513.

[16] Gao L, Chen X, Peng T, et al. Caveolin-1 protects against hepatic ischemia/reperfusion injury through ameliorating peroxynitrite-mediated cell death. Free Radic Biol Med. 2016;95:209-215.

[17] Deng GH, Wu CF, Li YJ, et al. Caveolin-1 is critical for hepatic iron storage capacity in the development of nonalcoholic fatty liver disease. Mil Med Res. 2023;10(1):53. Published 2023 Nov 8.

[18] Nagre N, Wang S, Kellett T, et al. TRIM72 modulates caveolar endocytosis in repair of lung cells. Am J Physiol Lung Cell Mol Physiol. 2016;310(5):L452-L464.

[19] Dong G, Ryan TE, Esser KA. Animal Models of Exercise and Cardiometabolic Disease.Circ Res. 2025, 137(2):139-162.

[20] Zhang Y, Wei H, Wang M, et al. Dexmedetomidine alleviates ferroptosis following hepatic ischemia-reperfusion injury by upregulating Nrf2/GPx4-dependent antioxidant responses.Biomed Pharmacother. 2023, 169:115915.

[21] Kamimura K, Yokoo T, Abe H, et al. Image-Guided Hydrodynamic Gene Delivery: Current Status and Future Directions. Pharmaceutics. 2015, 7(3):213-223.

[22] Kim HY. Statistical notes for clinical researchers: Two-way analysis of variance (ANOVA)-exploring possible interaction between factors. Restor Dent Endod. 2014, 39(2):143-147.

[23] Weisleder N, Takeshima H, Ma J. Mitsugumin 53 (MG53) facilitates vesicle trafficking in striated muscle to contribute to cell membrane repair. Commun Integr Biol. 2009;2(3):225-226.

[24] Bian Z, Wang Q, Zhou X, et al. Sustained elevation of MG53 in the bloodstream increases tissue regenerative capacity without compromising metabolic function. Nat Commun. 2019;10(1):4659. Published 2019 Oct 11.

[25] Shu T, Zeng X, Wang J, et al. MG53 mediates skeletal muscle-liver cross-talk and enhances alcohol metabolism in alcoholic liver disease. Nat Commun. 2026;17(1):2722. Published 2026 Feb 13.

[26] Yamada N, Karasawa T, Wakiya T, et al. Iron overload as a risk factor for hepatic ischemia-reperfusion injury in liver transplantation: Potential role of ferroptosis. Am J Transplant. 2020;20(6):1606-1618.

[27] Li C, Wu Y, Chen K, et al. Gp78 deficiency in hepatocytes alleviates hepatic ischemia-reperfusion injury via suppressing ACSL4-mediated ferroptosis. Cell Death Dis. 2023;14(12):810. Published 2023 Dec 8.

[28] Li Z, Lu S, Qian B, et al. Sex differences in hepatic ischemia–reperfusion injury: a cross-sectional study. Sci Rep. 2023;13(1):5724. Published 2023 Apr 7.

[29] Dong J, Ke MY, Wu XN, et al. SRY is a Key Mediator of Sexual Dimorphism in Hepatic Ischemia/Reperfusion Injury. Ann Surg. 2022;276(2):345-356.

[30] Li S, Hu X, Yan X, et al. Daidzein attenuates hepatic ischemia/reperfusion injury via HMGB1-TLR4 signaling pathway. Toxicon. 2026;275:109042.

[31] Parton RG, del Pozo MA. Caveolae as plasma membrane sensors, protectors and organizers. Nat Rev Mol Cell Biol. 2013;14(2):98–112.

[32] Cai C, Masumiya H, Weisleder N, et al. MG53 nucleates assembly of cell membrane repair machinery. Nat Cell Biol. 2009;11(1):56–64.

[33] Weisleder N, Takizawa N, Lin P, et al. Recombinant MG53 protein modulates therapeutic cell membrane repair in treatment of muscular dystrophy. Sci Transl Med. 2012;4(139):139ra85.

[34] Xu J, Chen S, Liu D, et al. Suppression of hepatocyte ferroptosis via USP19-mediated deubiquitination of SLC7A11 in ischemia-free liver transplantation. Adv Sci. 2025;12(6):e2406200.

[35] Bai C, Xiao P, Chen Y, et al. GPX4 promoter hypermethylation induced by ischemia/reperfusion injury regulates hepatocytic ferroptosis. J Clin Transl Hepatol. 2024.

[36] Kojima H, Hirao H, Kadono K, et al. Cold stress-induced ferroptosis in liver sinusoidal endothelial cells determines liver transplant injury and outcomes. JCI Insight. 2024;9(3):e174354.

[37] Chow LS, Gerszten RE, Taylor JM, et al. Exerkines in health, resilience and disease. Nat Rev Endocrinol. 2022;18(5):273–289.

Figure legend

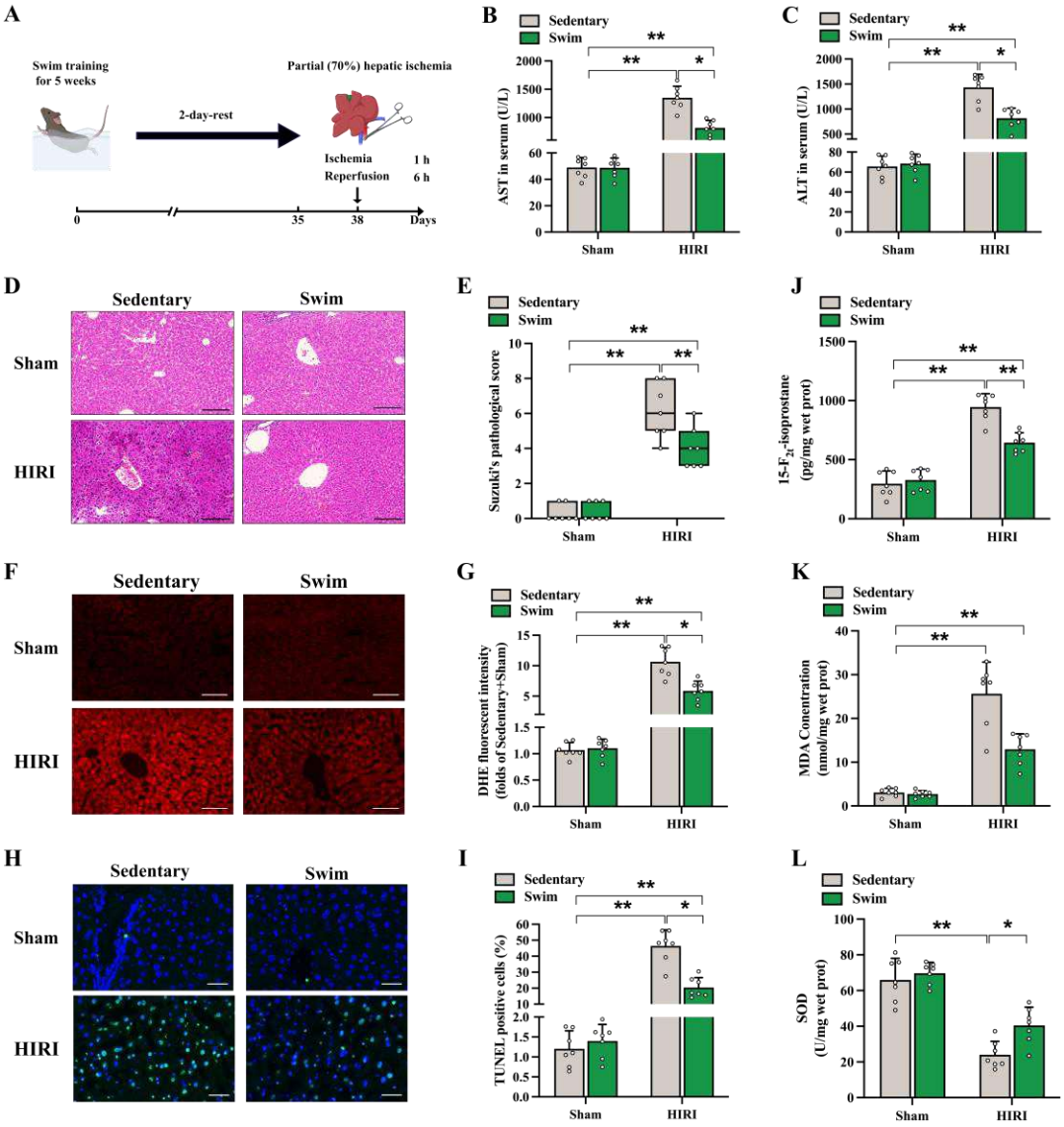


Fig. 1. Preoperative AET Protects Against HIRI by Attenuating Oxidative Stress and Apoptotic Cell Death.

(A) Experimental design: mice completed 5 weeks of swimming-based aerobic exercise training (AET), rested for 2 days, and then underwent 70% partial hepatic ischemia for 1 h followed by 6 h of reperfusion. (B, C) Serum aspartate aminotransferase (AST) and alanine aminotransferase (ALT) levels, respectively. (D) Representative hematoxylin and eosin (H&E)-stained liver sections (scale bar, 100 μm). (E) Suzuki histological injury scores. (F) Representative dihydroethidium (DHE)

fluorescence images of liver sections (red; scale bar, 100 μm). (G) Quantification of DHE fluorescence intensity. (H) Representative terminal deoxynucleotidyl transferase dUTP nick-end labeling (TUNEL) staining, showing TUNEL-positive cells (green) and DAPI-stained nuclei (blue) (scale bar, 50 μm). (I) Quantification of TUNEL-positive cells. (J) Hepatic 15-F2t-isoprostane levels. (K) Hepatic malondialdehyde (MDA) levels. (L) Hepatic superoxide dismutase (SOD) activity. Data are presented as mean ± SD (n = 7 per group). *$P < 0.05$; **$P < 0.01$.

Abbreviations: AET, aerobic exercise training; DHE, dihydroethidium; HIRI, hepatic ischemia–reperfusion injury; MDA, malondialdehyde; SOD, superoxide dismutase; TUNEL, terminal deoxynucleotidyl transferase dUTP nick-end labeling.

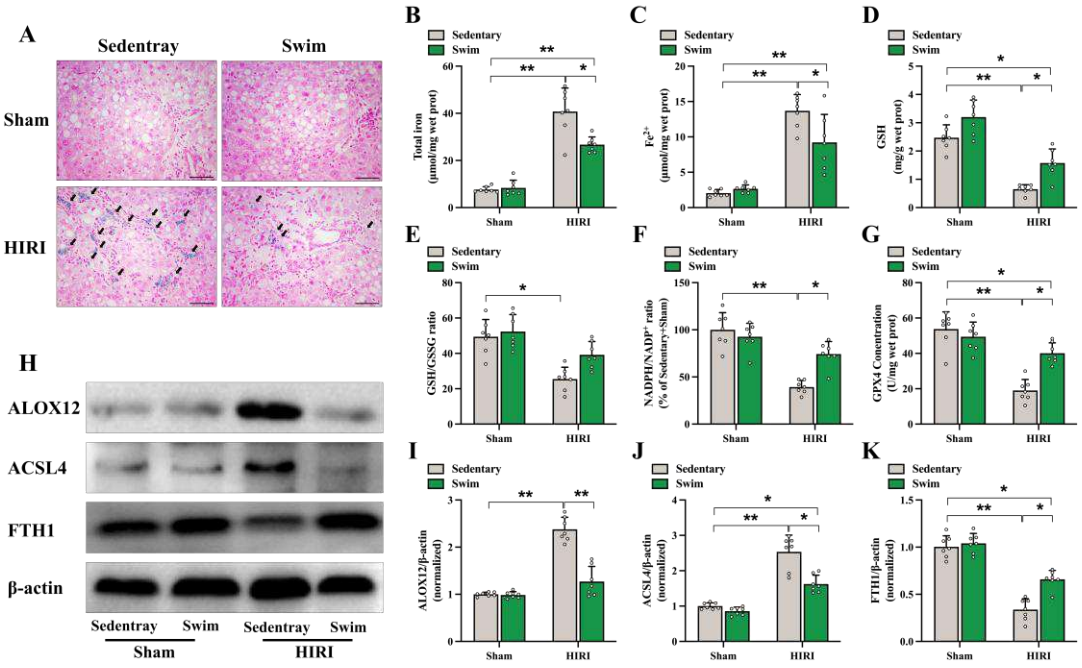


Fig. 2. Preoperative AET Attenuates Ferroptosis-Associated Iron Accumulation and Redox Imbalance During HIRI.

(A) Representative Prussian blue-stained liver sections; arrows indicate iron deposits (scale bar, 50 μm). (B, C) Hepatic total iron and ferrous iron (Fe^{2+}) levels, respectively. (D) Hepatic reduced glutathione (GSH) content. (E) GSH/oxidized glutathione (GSSG) ratio. (F) Reduced/oxidized nicotinamide adenine dinucleotide phosphate (NADPH/$NADP^+$) ratio. (G) Hepatic glutathione peroxidase 4 (GPX4) activity. (H) Representative immunoblots of ALOX12, ACSL4, and FTH1, with β-actin as the loading control. (I–K) Densitometric quantification of ALOX12, ACSL4, and FTH1, respectively, normalized to β-actin. Data are presented as mean ± SD (n = 7 mice per group). *$P < 0.05$; **$P < 0.01$.

Abbreviations: ACSL4, acyl-CoA synthetase long-chain family member 4; AET, aerobic exercise training; ALOX12, arachidonate 12-lipoxygenase; FTH1, ferritin heavy chain 1; GPX4, glutathione peroxidase 4; GSH, reduced glutathione; GSSG, oxidized glutathione; HIRI, hepatic ischemia–reperfusion injury; $NADP^+$, oxidized nicotinamide adenine dinucleotide phosphate; NADPH, reduced nicotinamide adenine dinucleotide phosphate.

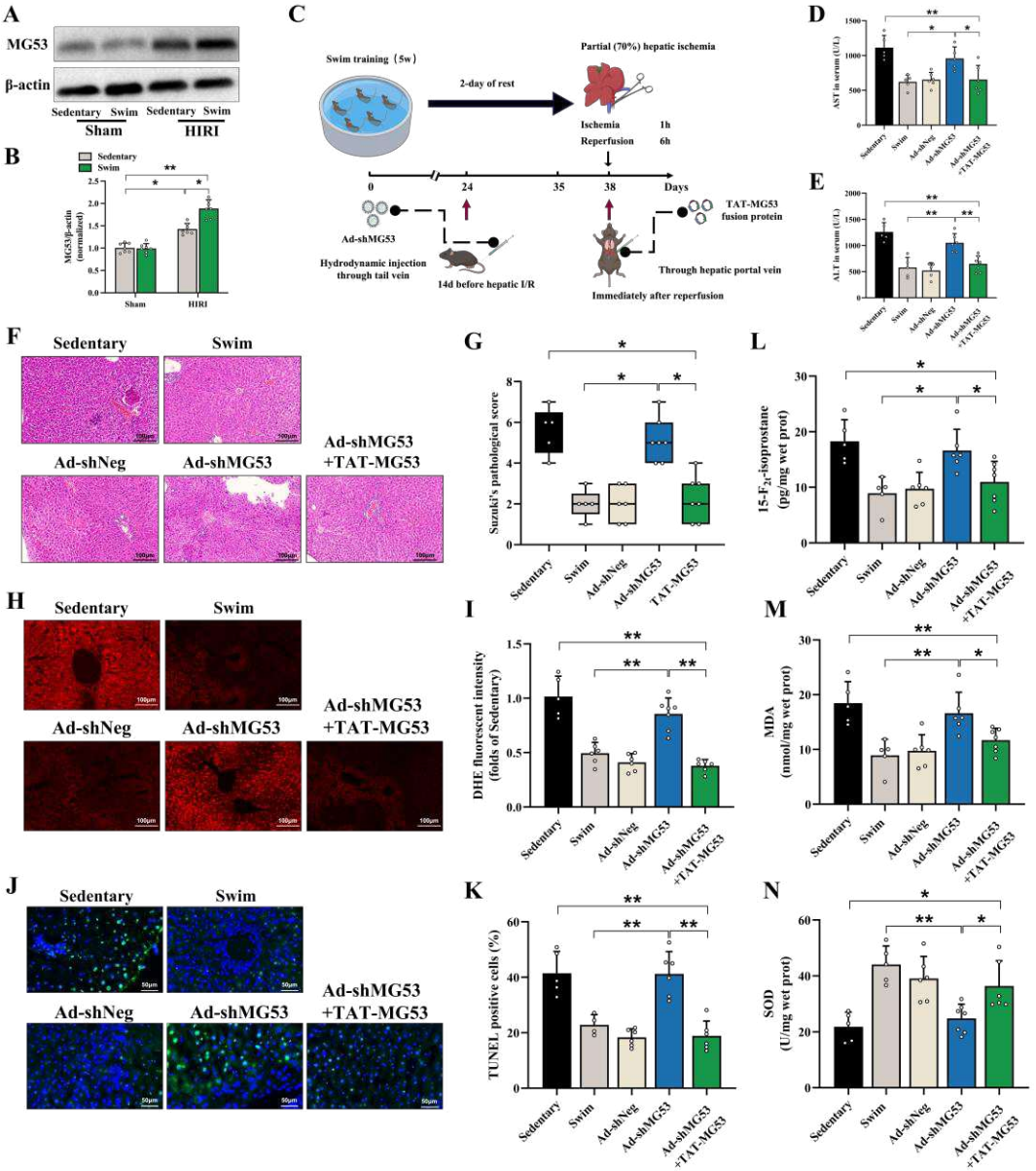


Fig. 3. MG53 Is Essential for AET-Mediated Hepatoprotection Against HIRI.

(A) Representative immunoblots of hepatic MG53. (B) Densitometric quantification of MG53 normalized to β-actin. (C) Experimental design: Ad-shMG53 was delivered by hydrodynamic tail-vein injection 14 days before hepatic ischemia–reperfusion (I/R), and TAT–MG53 was administered through the portal vein immediately after reperfusion. (D, E) Serum AST and ALT levels, respectively. (F) Representative H&E-stained liver sections (scale bar, 100 μm). (G) Suzuki histological injury scores. (H) Representative DHE fluorescence images of liver sections (red; scale bar, 100 μm). (I) Quantification of DHE fluorescence intensity. (J) Representative TUNEL staining, showing TUNEL-positive cells (green) and DAPI-stained nuclei (blue) (scale bar, 50 μm). (K) Quantification of TUNEL-positive cells. (L) Hepatic 15-F_{2t}-isoprostane levels. (M) Hepatic MDA levels. (N) Hepatic SOD activity. Data are presented as mean ± SD (n = 7 per group). *P < 0.05; **P < 0.01.

Abbreviations: Ad-shMG53, adenovirus encoding MG53-specific short hairpin RNA; Ad-shNeg,

negative-control adenovirus; AET, aerobic exercise training; DHE, dihydroethidium; HIRI, hepatic ischemia–reperfusion injury; I/R, ischemia–reperfusion; MDA, malondialdehyde; MG53, mitsugumin 53 (TRIM72); SOD, superoxide dismutase; TAT–MG53, transactivator of transcription–MG53 fusion protein; TUNEL, terminal deoxynucleotidyl transferase dUTP nick-end labeling.

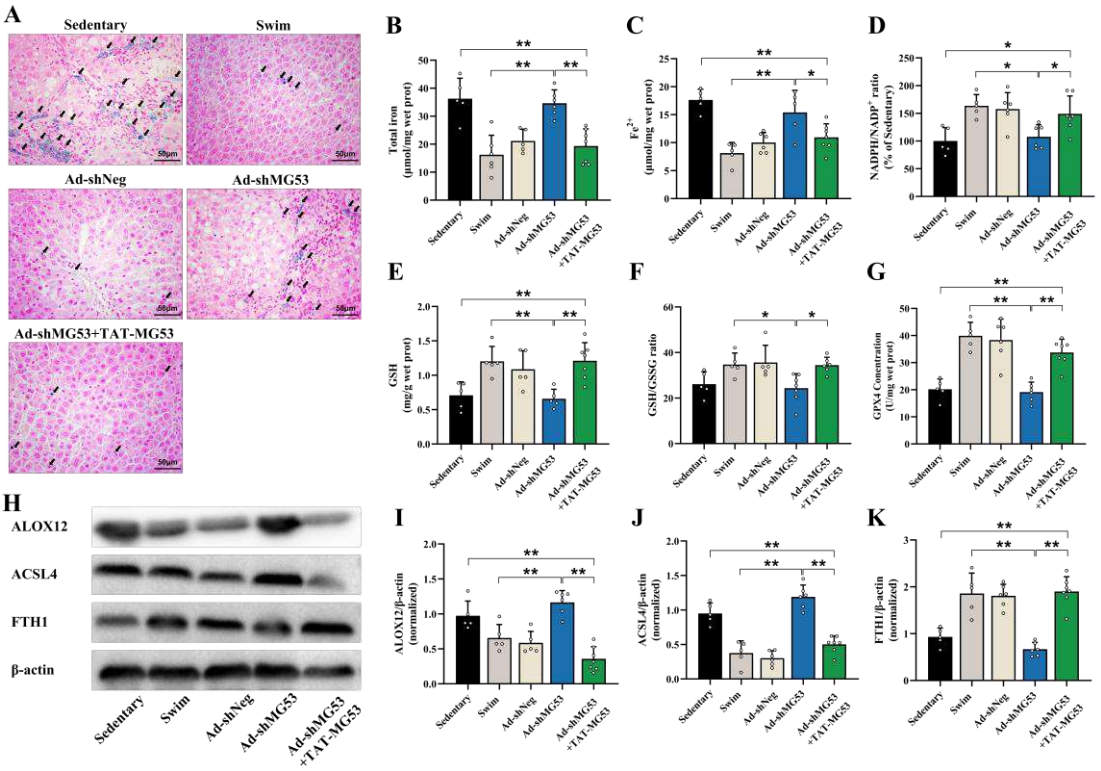


Fig. 4. MG53 Mediates the Protective Effects of AET on Hepatic Iron and Redox Homeostasis During HIRI.

(A) Representative Prussian blue-stained liver sections; arrows indicate iron deposits (scale bar, 50 μm). (B, C) Hepatic total iron and Fe^{2+} levels, respectively. (D) Hepatic NADPH/$NADP^+$ ratio. (E) Hepatic GSH content. (F) GSH/GSSG ratio. (G) Hepatic GPX4 activity. (H) Representative immunoblots of ALOX12, ACSL4, and FTH1, with β-actin as the loading control. (I–K) Densitometric quantification of ALOX12, ACSL4, and FTH1, respectively, normalized to β-actin. Data are presented as mean ± SD (n = 5–7 mice per group). *$P < 0.05$; **$P < 0.01$.

Abbreviations: ACSL4, acyl-CoA synthetase long-chain family member 4; Ad-shMG53, adenovirus encoding MG53-specific short hairpin RNA; Ad-shNeg, negative-control adenovirus; AET, aerobic exercise training; ALOX12, arachidonate 12-lipoxygenase; FTH1, ferritin heavy chain 1; GPX4, glutathione peroxidase 4; GSH, reduced glutathione; GSSG, oxidized glutathione; HIRI, hepatic ischemia–reperfusion injury; MG53, mitsugumin 53 (TRIM72); $NADP^+$, oxidized nicotinamide adenine dinucleotide phosphate; NADPH, reduced nicotinamide adenine dinucleotide phosphate; TAT–MG53, transactivator of transcription–MG53 fusion protein.

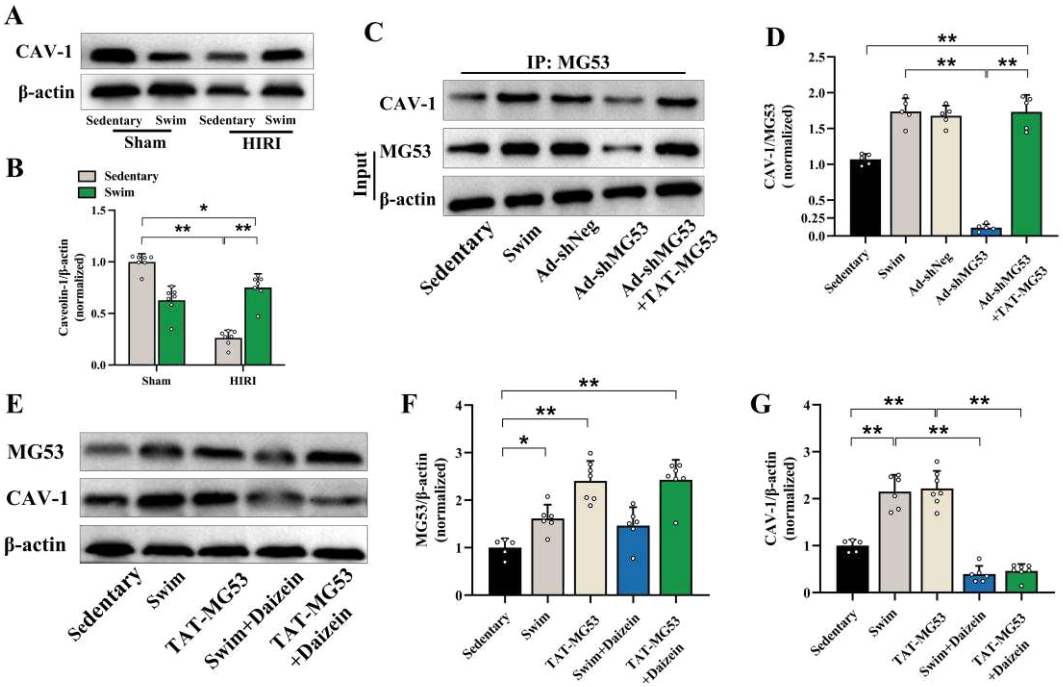


Fig. 5. Preoperative AET Enhances the Hepatic MG53–CAV-1 Association During HIRI.

(A) Representative immunoblots of hepatic caveolin-1 (CAV-1) in sedentary and AET-trained mice after sham surgery or HIRI. (B) Densitometric quantification of CAV-1 normalized to β-actin. (C) Representative co-immunoprecipitation analysis of the hepatic MG53–CAV-1 association. CAV-1 was detected after MG53 immunoprecipitation; input lysates were immunoblotted for MG53 and β-actin. (D) Quantification of co-immunoprecipitated CAV-1 normalized to MG53. (E) Representative immunoblots of hepatic MG53 and CAV-1 after AET, TAT–MG53 administration, and/or daidzein treatment. (F, G) Densitometric quantification of MG53 and CAV-1, respectively, normalized to β-actin. Data are presented as mean ± SD (n = 5–7 mice per group). **P* < 0.05; ***P* < 0.01.

Abbreviations: AET, aerobic exercise training; CAV-1, caveolin-1; HIRI, hepatic ischemia–reperfusion injury; MG53, mitsugumin 53 (TRIM72); TAT–MG53, transactivator of transcription–MG53 fusion protein.

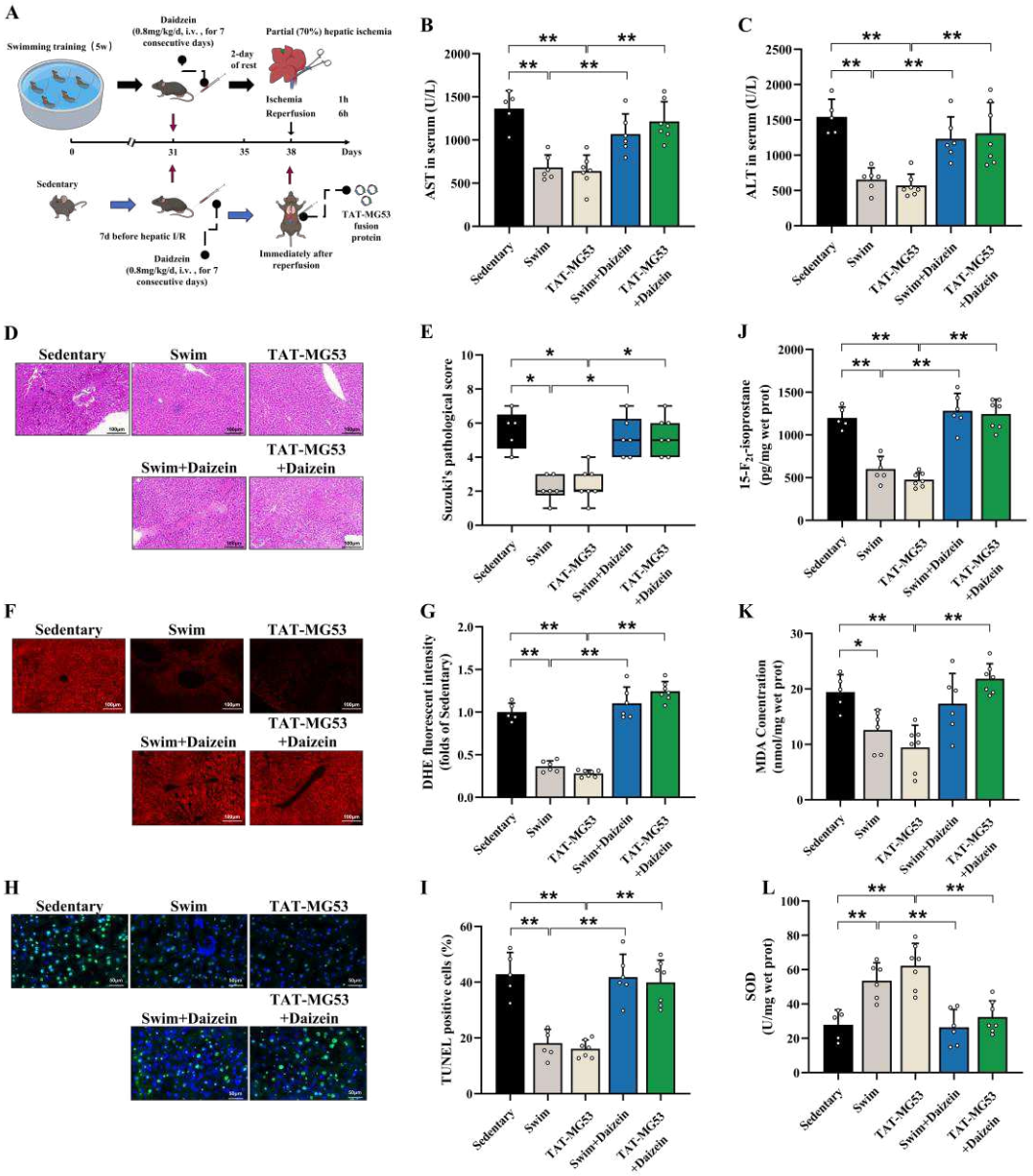


Fig. 6. Pharmacological Suppression of CAV-1 Abrogates AET- and MG53-Mediated Hepatoprotection Against HIRI.

(A) Experimental design: sedentary or AET-trained mice received daidzein (0.8 mg/kg/day, intravenously) for 7 consecutive days before hepatic I/R; TAT–MG53 was administered through the portal vein immediately after reperfusion. (B, C) Serum AST and ALT levels, respectively. (D) Representative H&E-stained liver sections (scale bar, 100 μm). (E) Suzuki histological injury scores. (F) Representative DHE fluorescence images of liver sections (red; scale bar, 100 μm). (G) Quantification of DHE fluorescence intensity. (H) Representative TUNEL staining, showing TUNEL-positive cells (green) and DAPI-stained nuclei (blue) (scale bar, 50 μm). (I) Quantification of TUNEL-positive cells. (J) Hepatic 15-F_{2t}-isoprostane levels. (K) Hepatic MDA levels. (L) Hepatic SOD activity. Data are presented as mean ± SD (n = 5–7 mice per group). *P < 0.05; **P < 0.01.

Abbreviations: AET, aerobic exercise training; CAV-1, caveolin-1; DAPI, 4′,6-diamidino-2-phenylindole; DHE, dihydroethidium; HIRI, hepatic ischemia–reperfusion injury;

I/R, ischemia–reperfusion; MDA, malondialdehyde; MG53, mitsugumin 53 (TRIM72); SOD, superoxide dismutase; TAT–MG53, transactivator of transcription–MG53 fusion protein; TUNEL, terminal deoxynucleotidyl transferase dUTP nick-end labeling.

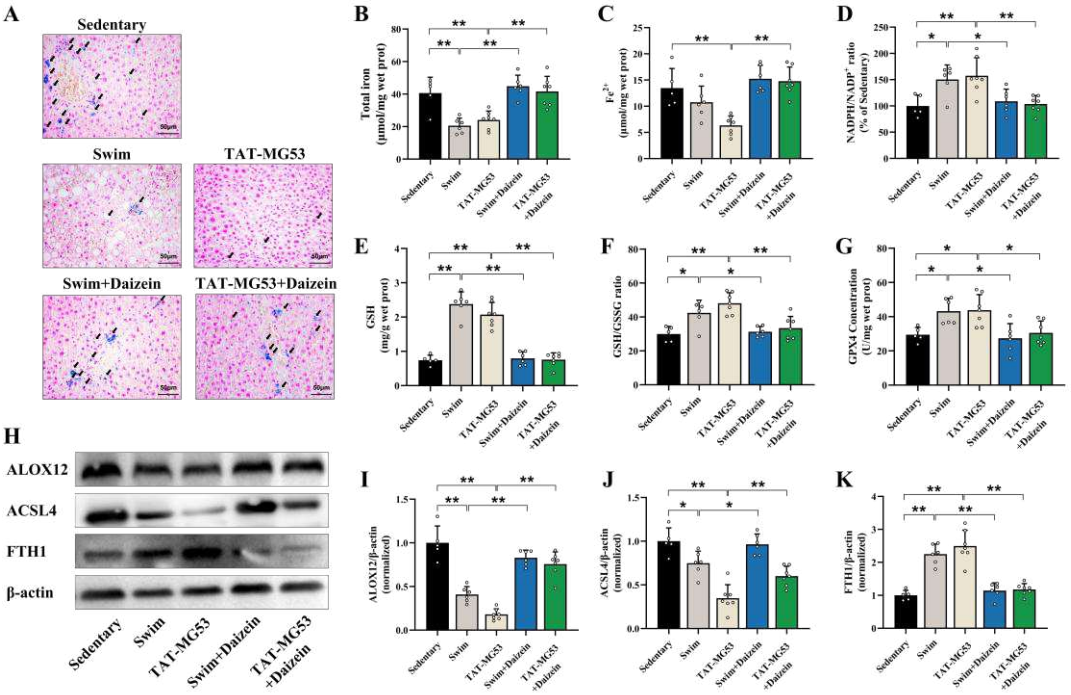
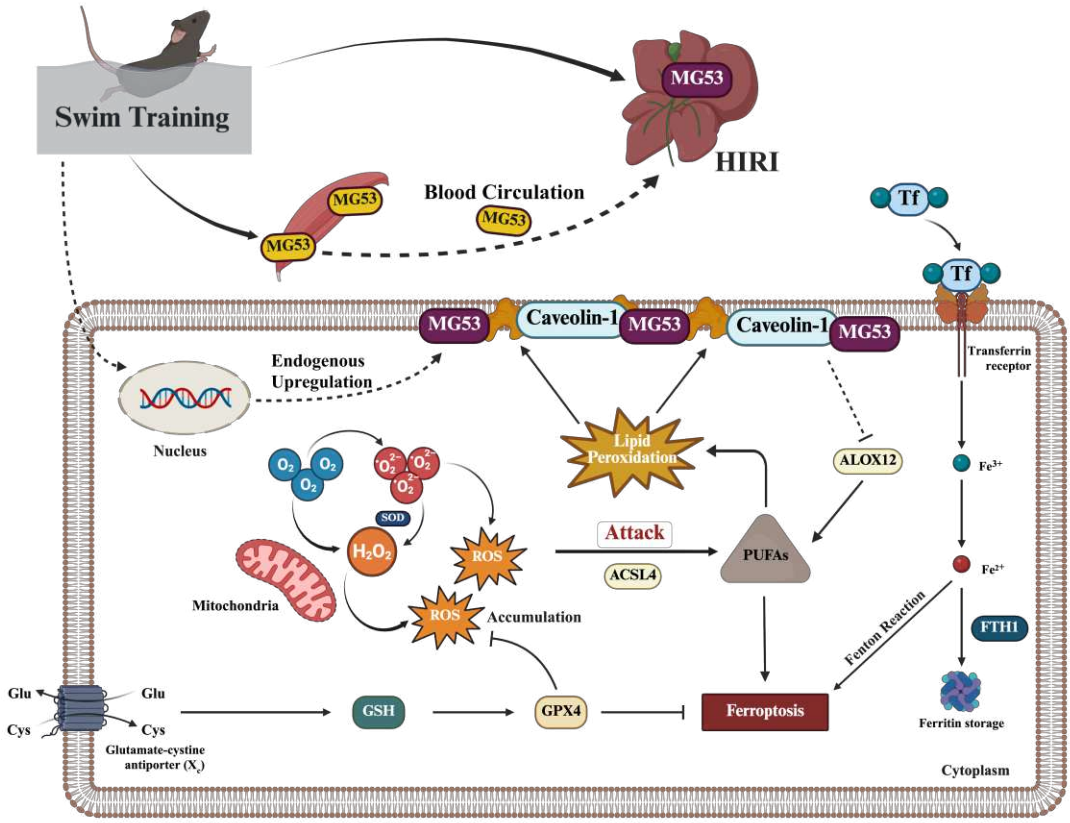


Fig. 7. CAV-1 Suppression Reverses AET- and MG53-Mediated Improvements in Hepatic Iron and Redox Homeostasis During HIRI.

(A) Representative Prussian blue-stained liver sections; arrows indicate iron deposits (scale bar, 50 μm). (B, C) Hepatic total iron and Fe^{2+} levels, respectively. (D) Hepatic NADPH/$NADP^+$ ratio. (E) Hepatic GSH content. (F) GSH/GSSG ratio. (G) Hepatic GPX4 activity. (H) Representative immunoblots of ALOX12, ACSL4, and FTH1, with β-actin as the loading control. (I–K) Densitometric quantification of ALOX12, ACSL4, and FTH1, respectively, normalized to β-actin. Data are presented as mean ± SD (n = 5–7 mice per group). *$P < 0.05$; **$P < 0.01$.

Abbreviations: ACSL4, acyl-CoA synthetase long-chain family member 4; AET, aerobic exercise training; ALOX12, arachidonate 12-lipoxygenase; CAV-1, caveolin-1; FTH1, ferritin heavy chain 1; GPX4, glutathione peroxidase 4; GSH, reduced glutathione; GSSG, oxidized glutathione; HIRI, hepatic ischemia–reperfusion injury; MG53, mitsugumin 53 (TRIM72); $NADP^+$, oxidized nicotinamide adenine dinucleotide phosphate; NADPH, reduced nicotinamide adenine dinucleotide phosphate; TAT–MG53, transactivator of transcription–MG53 fusion protein.



Graphical Abstract. Proposed model of MG53–CAV-1-mediated protection against hepatic ischemia–reperfusion injury.

Preoperative AET increases hepatic MG53 abundance. The source of this increase remains to be clarified and may involve enhanced uptake of circulating MG53 released from skeletal muscle and/or exercise-induced upregulation within hepatocytes. In the liver, MG53 functionally associates with Caveolin-1, and this interaction is required for AET-mediated hepatoprotection. Both AET and exogenous MG53 supplementation attenuate hepatic I/R injury, whereas Caveolin-1 inhibition abolishes this protective effect, indicating that MG53-dependent hepatoprotection requires intact Caveolin-1. The MG53-Caveolin-1 axis mitigates oxidative stress and restrains ferroptosis through multiple coordinated mechanisms: (i) limiting hepatic iron accumulation; (ii) restoring glutathione and NADPH redox balance and sustaining GPX4 activity; (iii) suppressing ferroptosis-associated enzymes ALOX12 and ACSL4; and (iv) maintaining FTH1 expression to facilitate iron sequestration. Collectively, these processes preserve redox homeostasis and reduce ferroptotic hepatocyte death during reperfusion. Dashed arrows denote literature-supported or inferred links not directly examined in this study.

Abbreviations: AET, aerobic exercise training; HIRI, hepatic ischemia/reperfusion injury; MG53, mitsugumin-53; GPX4, glutathione peroxidase-4; GSH, reduced glutathione; ROS, reactive oxygen species; ACSL4, acyl-CoA synthetase long-chain family member-4; ALOX12, arachidonate 12-lipoxygenase; FTH1, ferritin heavy chain-1; Tf, transferrin; PUFA, polyunsaturated fatty acid.

Supplementary Files

This is a list of supplementary files associated with this preprint. Click to download.

- SupplementWBRawBands.pdf
- Rawdata.zip
- supplementmaterials.docx